

Quantification of Damage Progression in a Thermally Aged Duplex Stainless Steel

A. Hazarabedian^{a*}, and B. Marini^b

^a DM / CAC / CNEA

Av. del Libertador 8250. Buenos Aires. (1430) Argentine

^b Commissariat à l'Énergie Atomique, DEN/DMN/SRMA,

Gif-sur-Yvette, 91191 France

Received: August 17, 2001; Revised: April 29, 2002

Ferrite of austeno-ferritic stainless steels maintained for a long time at temperatures in the range of 270 °C to 400 °C is embrittled like the known 475 °C embrittlement of ferritic stainless steels. Deformation and damage micromechanisms of a material must be known in order to apply the “local approach to fracture” (LAF) methodology. In this work we test a previous model of damage nucleation and evolution, extending its validity to low temperature - long term aging. We have determined cracking damage evolution by taking replicas of planar tensile specimens during uniaxial traction tests. Voronoï (Dirichlet) tessellation quantitative metallography was applied to characterize and quantify non-uniform damaging. Clustering criteria allowed the determination of the size, density and internal damaging rate of damage clusters.

Keywords: duplex austeno-ferritic stainless steel, thermal aging, metallography, Voronoï

1. Introduction

Corrosion resistant stainless steels (ASTM CF3, CF8 and CF8M) are widely used in cast components of the primary circuit of nuclear power plants. These steels have a duplex ferrite - austenite microstructure. After a long time operation, (greater than 10000 h) at hot branch temperatures (approx. 325 °C) or cold branch temperatures (280 °C), these materials suffer an aging phenomenon¹, similar to the 475 °C embrittlement of ferritic stainless steels². Aging hardens the ferrite, and consequently the overall hardness and strength increase. However ductility, toughness and impact resistance decrease, ductile-brittle transition shifts to higher temperatures and the upper shelf energy lowers. To assess a component's remaining life, it is necessary to determine the amount of the degradation of the mechanical properties, fracture toughness in particular. The thermal aging of cast duplex stainless steels depends on many factors. The most reported are the ferrite content, thermal history, microstructure, chemical composition and texture. Experimental results present a wide scatter that difficults the task of predicting a component state from a laboratory study. To deal with this problem, methods based on the local approach to fracture³ have been implemented. This approach, requires

the quantitative knowledge of the damage nucleation rate.

Damage and fracture mechanisms of aged duplex stainless steels are known and well documented in the literature⁴. Ferrite is hardened as a consequence of the precipitation of ordered Cr rich phases or by spinodal decomposition. Hardening promotes strain localization and the premature cracking of ferrite islands. This cracks eventually became cavities that lead to the final ductile fracture by cavity growth and coalescence. Joly³ showed that this damage is not uniformly distributed. Some regions are more prone to fracture. These regions have the size of the ferritic packet (in the order of 0.5 mm³) and belong to regions where crystallographic orientation favors the cracking process. In particular, packets oriented in such a way that only one slip system is activated are much more damaged than the rest. The size, distribution, and damage rate inside these regions control the overall ductility.

Because final fracture is ductile, the material is described using an elastoplastic porous model, (Gurson – Tvergaard⁵). The yield stress in this model is given by:

$$\sigma_{eq}^2(\epsilon_{eq}^p) = \sigma_y^2(\epsilon_{eq}^p) \sqrt{1 - 2f(\epsilon_{eq}^p)q_1 \cosh\left[\frac{3\sigma_m(\epsilon_{eq}^p)}{2\sigma_y}\right]} \quad (1)$$

*e-mail: hazarabe@cnea.gov.ar

Trabalho apresentado no IV Colóquio Latinoamericano de Fractura y Fatiga

where f is the volume fraction of porosity, q_1 is a constant equal to 1,5, σ_m , σ_y and σ_{eq} are the hydrostatic, yield and equivalent stresses respectively and ϵ_{eq}^p is the equivalent plastic deformation. In ferritic steels, cavities nucleate exclusively at the onset of plastic deformation and only its subsequent growth produce the critical condition for the fracture. This is why in many Gurson model implementations the nucleation term is not included. Joly³ includes the nucleation term, when he applies this model to the case of aged duplex stainless steels. He found that the number of cracks is proportional to the plastic deformation. The proposed equation governing porosity was:

$$\frac{df(\epsilon_{eq}^p)}{d\epsilon_{eq}^p} = f q_1 \frac{3}{2} \cosh\left[\frac{3}{2} \frac{\sigma_m}{\sigma_0}\right] + A_n \quad (2)$$

where A_n , the crack nucleation rate, is the unique parameter required by the model, besides the standard tensile curve. Following Joly's idea, we assume that the crack nucleation rate is a random value, corresponding to an uniform value in a segment and null outside.

This model was developed studying the damage and fracture mechanisms of accelerated aged duplex steels. However, it has been proved that at temperatures above 350 °C the predominant aging mechanism is the precipitation of the Cr rich α' phase and at temperatures below 350 °C, ferrite suffers spinodal decomposition. It is necessary to prove its validity to realistic aging conditions. Thus, our first objective is to check if the deformation and damage mechanisms reported into literature for the high temperature – short term aged samples, are the same for our low temperature – long term laboratory-aged material. The second, is to get a formulation for A_n , obtaining parameters characterizing the inhomogeneous distribution of damage. A metallographic methodology, slightly different from the used by Joly will be developed for this objective, and applied to the F32 alloy aged 30000 hours at 350 °C. The parameters obtained will be used to calculate the fracture toughness of one of the aged conditions in the second part of this work⁶.

2. Experimental

Materials and heat treatments

Because at equal thermal history, aging of duplex steels depends on the ferrite content, we have studied three steels, having 8% (low), 20% (average) and 32% (high, out of specification) ferrite (δ). These heats were produced with the same method used for the actual reactor's components. Ferrite content was determined by a magnetic method. Table 1 gives alloy's compositions and ferrite contents.

As the aging depends on the time and temperatures at which the material remained, we will describe results of

Table 1. Composition and ferrite content of materials.

Material	C	Cr	Ni	Mo	Mn	Si	N ₂ (ppm)	δ
F8	0.029	18.13	8.3	0.57	0.52	1.34	330	8%
F20	0.023	20.48	10.01	2.50	0.87	0.90	530	20%
F32	0.033	22.28	9.92	2.34	0.91	0.86	510	32%

Table 2. Aging heat treatments.

Code	Temperature	Time
T0	Room	Undefined
T1	325 °C	30000 h
T2	400 °C	3000 h

different aging treatments. The portability of the models developed for the high temperature accelerated treatments to the realistic low temperature - large time aged condition will be emphasized. Table 2 describes their identification.

3. Mechanical properties

Tensile properties were obtained from standard cylindrical specimens (NF EN 10002-1) of 8 mm diameter and 40 mm gauge length.

Damage progression study

Studies, by optical and electron microscopy, were performed on longitudinal cuts of tensile specimens tested in different aged conditions, in order to verify the deformation, damage and fracture mechanisms described in the literature for these materials.

Because damage is inhomogeneous, it is necessary to identify the sites more susceptible to crack. For this objective, we have used a replica technique. A new set of uniaxial tensile tests was performed, on specimens having an 8 mm x 6 mm rectangular section. One of its largest sides was polished and etched to reveal material's microstructure. At regular intervals during straining, the test was interrupted to take a replica. In this way, we obtained 15 to 20 records of the damage evolution. This allowed us to focus the damage study at the site of the greatest interest: the surroundings of the weakest site, where fracture actually took place.

To count the cracks, we manually processed images in order to mark a point where a crack was present. An automatic analysis will mark as cracks any artifact (dark stains, polymer cracks or other defects) that the replica presents. These artifacts are absent in the specimen. In this way, any indication in the replica uncorrelated to a crack on the specimen was neglected. A data processing based on Voronoi cells and Delaunay triangulation⁷ (Fig. 5) was used to quantify the spatial distribution and the local density of cracks.

Using the Delaunay triangulation, the distance of each crack to its neighbors is determined. To elucidate if a crack belongs or not to a cluster, (a cluster indicates a damage

susceptible region) a distance and local density based criterion has been established. A crack belongs to a cluster if the distance to its neighbors is lower than the mean distance between cracks, and its local density is greater than the global density. In this way, several quantities that characterize crack clustering can be obtained: The number of cracks in the i -th cluster is noted n_i , the surface of the i -th cluster S_i , is defined as the sum of the areas of the cells enclosing the cracks forming that cluster. G is the mean volume of cavities and ϵ is the plastic deformation. The parameters needed for the numeric simulations are calculated using the set of equations 3. We define the probability ϕ of a volume element of being a crack susceptible site as the ratio of the sum of the measured clusters areas to the total area of observation S_{total} . The size (V_0) of a volume representative element can be obtained transforming the mean value of the cluster surface.

$$\bar{A} = \frac{1}{\epsilon} \frac{G \sum_i n_i}{\sum_i S_i}, \quad \phi = \frac{\sum_i S_i}{S_{total}} \quad \text{and} \quad V_0 = (\bar{S})^{3/2} \quad (3)$$

We assign \bar{A} to the mean value of the A_n distribution. It is worth nothing that it is proportional to the quotient between the total number of “clustered” cracks and the total cluster area. We found that Joly’s approach (\bar{A} proportional to the mean value of (n_i/S_i)), overestimates the crack nucleation rate. This is a consequence of the small size of S_i ’s, which are always presentation a random metallographic cut.

4. Results and Discussion

Figure 1 shows a section of the 32% ferrite specimen, aged 3000 h at 325 °C. In accordance with the literature,

we find that deformation is uniformly distributed into the austenite and is localized in narrow slip bands into the ferrite, giving a strong contrast (Fig. 2). In this micrograph three deformation systems of the ferrite phase could be easily recognized: two plane systems (whose bisector contains a crack) and a pencil glide system.

It was observed that cracks nucleated continuously during the test and were not uniformly distributed. Furthermore, they were localized in several ferrite packets. The cracking mechanism was by cleavage or by shear of the

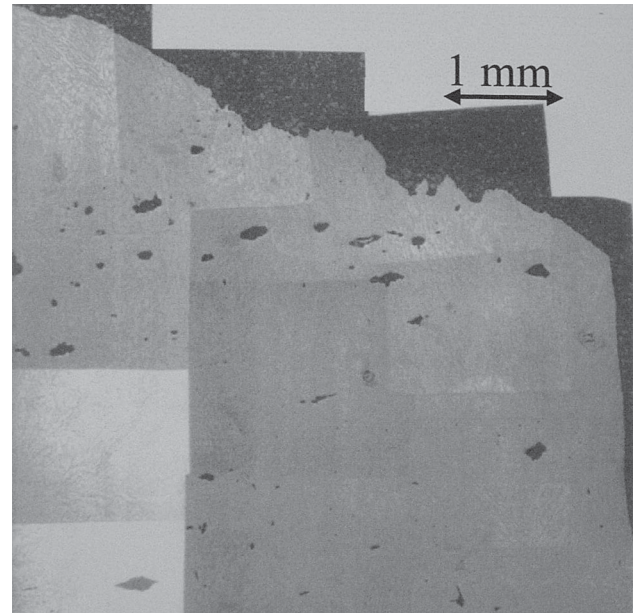


Figure 1. metallographic cut of a F32 steel aged 3000 h at 325 °C and strained to fracture.

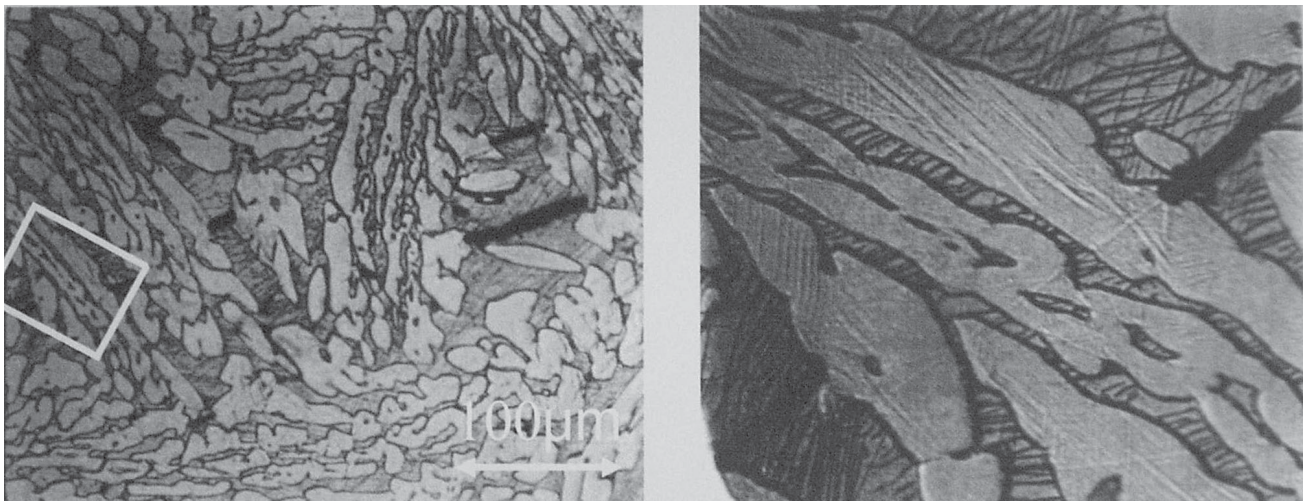


Figure 2. Deformation and cracking of a F32 T1 unnotched specimen after fracture. A magnified detail can be seen at right.

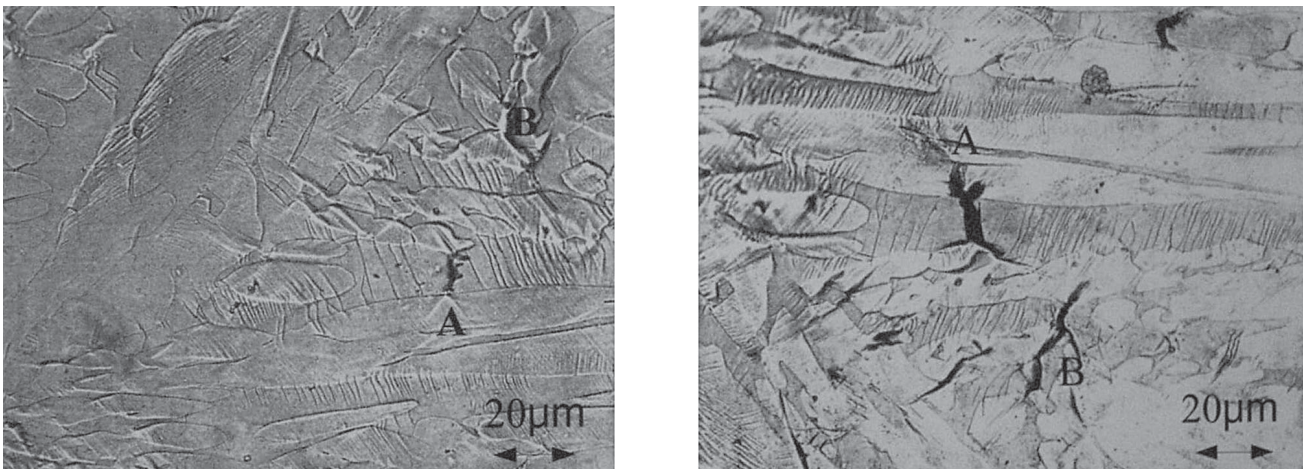


Figure 3. Damage progression. Left photograph shows a replica taken at 6% of plastic deformation. Right photograph shows the same region on the specimen after rupture (12% deformation). A and B indicates the same crack on the two slides.

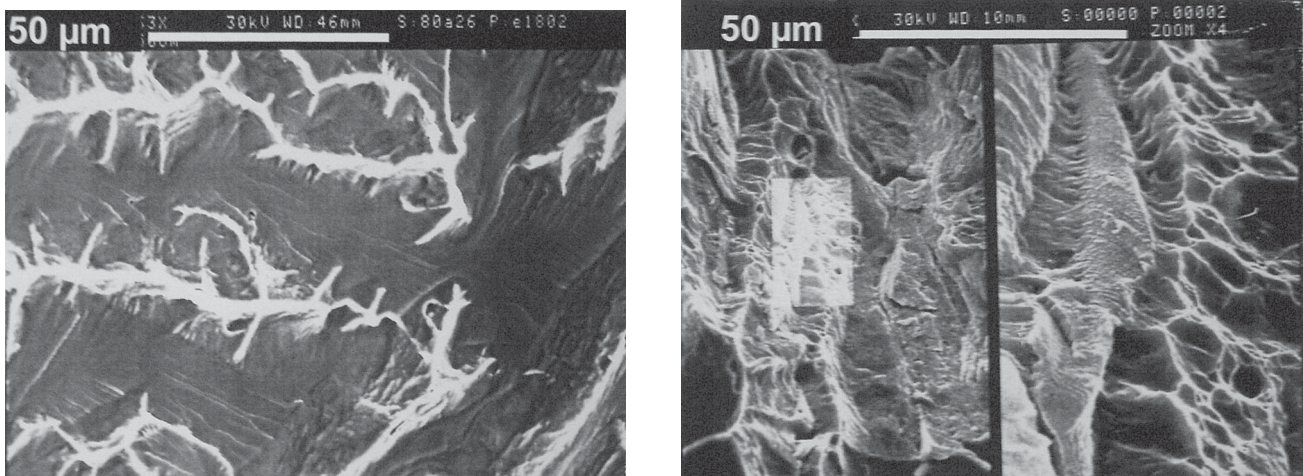


Figure 4. Fracture surface of aged material a) F32 Shows cleavage of the ferrite and necking of austenite b) F20 showing fragile shearing in ferrite and tearing of austenite.

ferritic laths. Cracks were locally parallel inside a packet. These cracks eventually became the cavities of the final fracture having ductile characteristics.

We have observed that the microcrack aperture is controlled by the local extent of deformation, increasing during the test, Fig. 3. We have also observed that for the F32 T1 material, the ferrite breaks by cleavage, but the ferrite of the F20 material fails generally by shear (Fig. 4).

Figure 5 contains the map of crack locations of a F20 specimen aged 10000 h at 400 °C. Fracture surface is at the upper side. Dots indicate the center of gravity of the cracks. The Delaunay triangulation is displayed only for the cracks which satisfy our criterion to form a cluster.

The Voronoï analysis for the F32 steel heat treatment gave the following results:

$$\bar{A} = 0.44; \phi = 0,063 \text{ and } V_0 = 42 \times 10^{-3} \text{ mm}^3$$

These parameters will be used in the second part of this work to evaluate the fracture toughness.

5. Conclusions

We checked that the deformation and fracture mechanisms of thermally aged duplex stainless reported in the literature are the same for our low temperature long - term aged alloys. A quantitative metallography method based on the Voronoï analysis allowed us to measure directly the size and density of the regions more susceptible to crack. Under the hypothesis of an uniform distribution of the crack nucleation rate inside these regions, the mean value of this

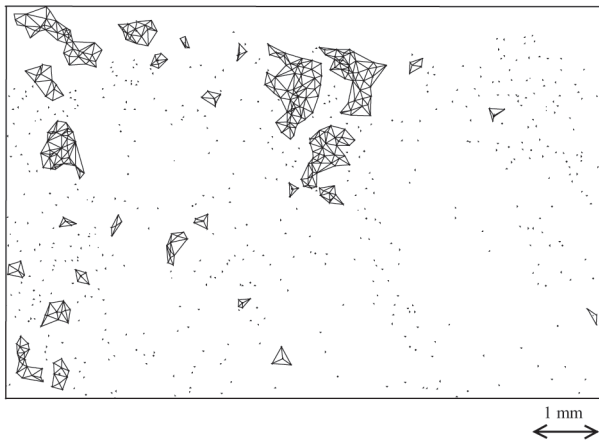


Figure 5. Crack map of a F20 (aged 10^4 h at $400\text{ }^\circ\text{C}$) specimen. Cracks are located at dots and at the vertices of triangles. Triangles show crack clusters from Voronoï analysis.

rate was obtained. We associate this quantity to the mean value of the crack nucleation rate occurring during the plastic deformation.

Acknowledgments

This work was performed during a stay of A. Hazarabedian in the “Laboratoire des Études Mécaniques” of Commissariat à l’Énergie Atomique, DEN/DMN/SRMA

– Gif-sur-Yvette, 91191 - France, in the course of IAEA - CEA - CNEA. ARG/83 cooperation contract.

References

1. Slama, G.; Petrequin, P.; Mager, T. Effect of aging on mechanical properties of austenitic stainless steel castings and welds, presented at SMIRT Post-Conference Seminar, 1983.
2. Lacombe P.; Baroux B.; Beranger G. editores. “Les aciers inoxydables”. *Les éditions de physique*, Les Ulis, 1990.
3. Joly, P. Thèse doctoral “Étude de la rupture d’aciers inoxydables austéno-ferritiques moulés, fragilisés par vieillissement à $400\text{ }^\circ\text{C}$ ”, *École des Mines de Paris*. May 1982.
4. Chung H.M. Aging and life prediction of cast stainless steel components. *Intl J. Press. Vessel & Piping*, v. 50, p. 179-213, 1992.
5. Gurson, A.L. Continuum theory of ductile rupture by void nucleation and growth: Part 1 - Yield criteria and flow rules for porous ductile media, *J. of Eng. Mat & Tech.*, v. 99, p. 2-15, 1997.
6. Tvergaard, V. On localization in ductile materials containing spherical voids. *Intl. J. of Fracture*, v. 18, p. 237-252, 1982.
7. Hazarabedian, A.; Forget, P.; Marini, B. Local approach to fracture of an aged duplex stainless steel, *Mat. Res.*, v. 5, n. 2, p. 131-135, 2002.
8. Bauvineau, Laurent. Approche locale de la rupture ductile: Application à un acier Carbone - Manganèse. Thèse de doctorat. *École des Mines de Paris*. Dic. 1996.